

Zero-metallicity stars

II. Evolution of very massive objects with mass loss

P. Marigo¹, C. Chiosi¹, R.-P. Kudritzki²

¹ Dipartimento di Astronomia, Università di Padova, Vicolo dell’Osservatorio 2, I-35122 Padova, Italy

² Institute for Astronomy, University of Hawaii, 2680 Woodlawn Drive, Honolulu, HI 96822

Received September 19, 2002 / Accepted November 26, 2002

Abstract. We present evolutionary models of zero-metallicity very massive objects, with initial masses in the range $120 M_{\odot} - 1000 M_{\odot}$, covering their quiescent evolution up to central carbon ignition. In the attempt of exploring the possible occurrence of mass loss by stellar winds, calculations are carried out with recently-developed formalisms for the mass-loss rates driven by radiation pressure (Kudritzki 2002) and stellar rotation (Maeder & Meynet 2000). The study completes the previous analysis by Marigo et al. (2001) on the constant-mass evolution of primordial stars. Our results indicate that radiation pressure (assuming a minimum metallicity $Z = 10^{-4} \times Z_{\odot}$) is not an efficient driving force of mass loss, except for very massive stars with $M \gtrsim 750 M_{\odot}$. On the other hand, stellar rotation might play a crucial role in triggering powerful stellar winds, once the $\Omega\Gamma$ -limit is approached. However, this critical condition of intense mass loss can be maintained just for short, as the loss of angular momentum due to mass ejection quickly leads to the spinning down of the star. As by-product to the present work, the wind chemical yields from massive zero-metallicity stars are presented. The helium and metal enrichments, and the resulting $\Delta Y/\Delta Z$ ratio are briefly discussed.

Key words. Stars: evolution – Stars: interiors – Stars: Hertzsprung–Russell (HR) diagram – Stars: mass loss – Cosmology: early Universe

1. Introduction

The first generation of stars ever born in the Universe (Population III) is assigned a role of paramount importance for several astrophysical issues. In particular, the formation of a primeval population of very massive objects (VMOs, with initial masses in the range $10^2 - 10^5 M_{\odot}$) was invoked in the '80s to explain several questions, such as the observed metallicities of Population II stars, the primordial helium abundance, the re-ionisation of cosmic matter after the Big-Bang, the missing mass in clusters of galaxies and galactic haloes, the G-dwarf problem (see Carr et al. 1984 for an extensive review). In those years a few evolutionary calculations of zero-metallicity VMOs were carried out (e.g. Bond et al. 1984, El Eid et al. 1983, Ober et al. 1983, Klapp 1984ab), but afterwards the scientific production on the evolution of the first stars dropped off.

The recently renewed interest in Pop-III stars, essentially driven by the nowadays flourishing of observations at very low metallicity and/or high redshift (refer to e.g. the proceedings of the ESO symposium edit by Weiss et al. (2000); see also Kudritzki et al. (2000), Bromm et al. (2001), Schaerer (2002), Panagia (2002) for extensive analyses on the expected observ-

able properties of primordial stellar populations) has again stimulated the calculation of stellar structures made evolve with initial metal-free chemical composition (e.g. Cassisi et al. 2001; Marigo et al. 2001 and references therein).

Marigo et al. (2001; thereafter Paper I) presented an extensive study of the evolutionary properties of zero-metallicity stars over a wide range of initial masses ($0.7 M_{\odot} \lesssim M \lesssim 100 M_{\odot}$). In that work – to which the reader is referred for all the details – we calculated all stellar tracks at constant mass.

Our study on Pop-III stars is now extended to very massive objects (VMOs), with initial masses in the range $120 - 1000 M_{\odot}$, that is chosen not only for continuity with Paper I, but also in consideration of current theoretical indications that the primordial initial mass function (IMF) might have peaked in the (very) high-mass domain (with $M \gtrsim 100 M_{\odot}$; see e.g. Bromm et al. 1999, 2002; Nakamura & Umemura 2001; Abel et al. 2000).

To this aim we calculate evolutionary models for zero-metallicity VMOs that cover the major core-burning phases, extending from hydrogen to carbon ignition. With aid of available analytic formalisms, we address the question of the possible occurrence of mass loss via stellar winds, which is an important, but still problematic, aspect of stellar evolution at zero metallicity.

In massive stars with “normal” chemical composition the principal driving force resides in the capability of metallic ions, present in the atmosphere, to absorb radiative momentum and transfer it to the outermost layers, that can be then accelerated beyond their escape velocity (Castor et al. 1975; Pauldrach et al. 1986). In a gas composed only of hydrogen and helium, like the primordial one, the lack of metallic ions sets the first important difference and the question arises: Is the radiative acceleration due to the H and He lines strong enough to trigger significant mass loss? Furthermore, may other possible processes – e.g. related to pulsation instability and stellar rotation – be efficient mechanisms to drive mass loss from Pop-III massive stars?

Some of these questions have already been addressed by other investigations, others still deserve to be quantitatively analysed and discussed. There are few studies in the literature that present evolutionary models of very massive zero-metallicity stars with mass loss during the pre-supernova phases. In the very massive domain ($500 - 1000 M_{\odot}$) Klapp (1983, 1984) carried out evolutionary calculations by adopting a simple empirical law for mass-loss (Barlow & Cohen 1977) – based on Galactic observations – that linearly scales with the stellar luminosity. On the basis of semi-analytical models of very massive objects (with masses $10^2 - 10^5 M_{\odot}$), Bond et al. (1984) argued that the same kind of dynamical instability arising in the H-burning shell of Population I models – which should cause the ejection of the entire envelope – might also affect Population III VMOs, depending on the actual abundance of the CNO catalysts in the H-shell. The evolution of zero-metallicity stars (with masses $80 - 500 M_{\odot}$) during the nuclear phases of H- and He-burning was calculated by El Eid et al. (1983) with the adoption of a semi-empirical relation to derive the mass loss rate (Chiosi 1981). Recently Baraffe et al. (2001, see also Heger et al. 2001) performed a linear stability analysis on metal-free very massive models (with masses $120 - 500 M_{\odot}$), and investigated the related possibility that mass loss may characterise the pulsation-unstable stages. Heger & Woosley (2002) calculated the evolution and nucleosynthesis of quite massive Population III stars (with masses $\sim 100 - 300 M_{\odot}$) including the final fate of the supernova event, but no mass-loss is assumed to occur during the hydrostatic phases of major nuclear burnings.

In the present work we attempt to further explore the issue of mass loss in primordial conditions, by carrying out new evolutionary calculations of zero-metallicity VMO with recently developed mass-loss formalisms, related to radiation pressure and stellar rotation.

The paper is organised as follows. Section 2 introduces new evolutionary calculations for zero-metallicity VMOs, having initial masses of $120, 250, 500, 750$, and $1000 M_{\odot}$. Mass loss is included with the adoption of recent analytic formalisms, namely: Kudritzki (2002) for radiation-driven mass loss, and Maeder & Meynet (2000) for the additional effect of stellar rotation. General characteristics of the models are analysed in relation to energetics, nuclear lifetimes, internal structure, surface and chemical properties. The efficiency of mass loss is discussed on the basis of the adopted formalisms. The corresponding predictions for the chemical yields, ejected via stellar

winds, are given in Sect. 3. In particular, the expected helium and metal enrichment, produced by a hypothetical burst of Pop-III star formation, is derived and discussed as a function of the involved parameters. In Sect. 4 we express a few concluding remarks. Finally, stellar isochrones for very young ages are presented in Sect. A.

2. Evolutionary calculations

We have carried out evolutionary calculations of zero-metallicity very massive objects (VMO) with initial masses of $120, 250, 500, 750$, and $1000 M_{\odot}$. All input physics are the same as those employed in Paper I – to which the reader is referred for all details – except for the applied overshoot scheme. Overshooting is allowed from the borders of the convective cores with the parameter $\Lambda_c = 0.5$ (following Bressan et al. 1981), whereas the classical Schwarzschild criterion is otherwise applied (i.e. convective shells and outer envelope). The evolution is followed starting from the zero-age main sequence (MS) up to the ignition of central carbon, i.e. covering the major stages of hydrogen and helium burning.

In order to estimate the efficiency of mass-loss via stellar winds in primordial VMOs, we adopt recently-developed analytic formalisms (Kudritzki 2002; Maeder & Meynet 2000), whose basic ingredients are summarised in the next sections.

2.1. Radiation-driven mass-loss rates

The role of radiation pressure – on the resonance lines of metallic ions like CIII, NeII, OII – in driving mass loss from massive stars has been a firm result of theoretical astrophysics since the pioneer works by Lucy & Solomon (1970), and Castor et al. (1975; CAK). In short, the crucial term determining the efficiency of mass loss by line driven winds is the radiative line acceleration, which is expressed in units of the Thomson acceleration via the so-called force multiplier. This latter, in turn, is suitably parametrised as $M[t(r)] = kt^{-\alpha}n^{\delta}$, where $t(r)$ – the Thomson optical depth parameter – is proportional to the number density of electrons, the Thomson cross-section, and the ratio between the local velocity of thermal motion to the spatial gradient of the stellar wind outflow velocity field; k represents the normalisation integral over the contribution of all photon absorbing spectral lines with different line strength; n is the ratio of the local number density of electrons to the local geometrical dilution factor of the radiation field; and finally α and δ are suitable exponents describing the optical depth and density dependence of the radiative line force (see CAK, Abbott 1982a, Pauldrach et al. 1986, Kudritzki, 1988, 1998, 2002 and references therein for more details). The quantities k, α, δ are known as the force multiplier parameters.

The expected dependence of radiative wind efficiency on metallicity (in the range from solar to 0.01 solar) has been investigated by e.g. Abbott (1982b), Kudritzki et al. (1987), Leitherer et al. (1992), Kudritzki & Puls (2000, and references therein), Vink et al. 2001. The mass-loss rates are predicted to decrease at lower metallicities as a power law following $(Z/Z_{\odot})^b$, with $b = 0.5 - 0.8$.

Kudritzki (2002) in his investigation of winds, ionising fluxes and spectra of very massive stars at very low metallicities has recently extended the analysis down to 0.0001 solar. These calculations introduce a new treatment of the radiative line force and are based on revised and updated atomic physics and line lists (see e.g. Puls et al. 2000 and references therein). Following a more realistic consideration of the line strength distribution function, the usual assumption of constant force-multiplier parameters (k , α , δ) throughout the atmosphere is replaced by the introduction of an explicit dependence of these parameters on optical depth and density. This improved treatment of the line force is needed at extremely low metallicity, because the depth dependence of the radiative acceleration differs significantly from the case of higher metallicity. As a consequence, a new elaborate algorithm to calculate the conditions at the critical point of the wind is also needed.

The results of Kudritzki's stellar wind calculations are fitted by means of analytic formulas, that give the mass-loss rate as a function of effective temperature, luminosity and metal abundance for very massive stars with masses above $100 M_{\odot}$:

$$\log \dot{M} = q_1([Z] - [Z]_{\min})^{0.5} + Q_{\min} \quad \text{in } M_{\odot} \text{ yr}^{-1} \quad (1)$$

where we define

$$q_1 = Q_0 - Q_{\min}(-[Z]_{\min})^{-0.5}, \quad [Z] = \log(Z/Z_{\odot}) \quad (2)$$

with Z being the metallicity (abundance in mass fraction). The quantities $[Z]_{\min}$, Q_{\min} , and Q_0 are expressed as polynomials of the luminosity, in the form

$$f = a_0 + a_1 \mathfrak{L} + a_2 \mathfrak{L}^2 \quad \text{with } \mathfrak{L} = \log(L/L_{\odot}) - 6.0. \quad (3)$$

The coefficients a_i are given as a function of the effective temperature (see table 3 in Kudritzki 2002), in the range from 40000 to 60000 K.

The above formalism is applied with the following assumptions:

- At any time the metallicity – that enters Eqs. (1)-(2) – is set $Z = \max(Z_{\min}, Z_{\text{eff}})$. This means that when evaluating the radiative mass-loss rate we do not assume a truly zero metal content, but the maximum between the lowest value in the validity range of Kudritzki's formula ($Z_{\min} = 10^{-4} \times Z_{\odot}$), and $Z_{\text{eff}} = 1 - X - Y$. This latter denotes the effective current metallicity, with X and Y being the hydrogen and helium abundances, respectively. In this way we may account, to a first approximation, for any possible surface enrichment in metals (mainly CNO elements, such that $Z_{\text{eff}} > Z_{\min}$) exposed to the surface by stellar winds or convective mixing.
- For $T_{\text{eff}} > 60000$ K, we choose not to extrapolate the fit formula beyond its validity domain, but constrain $T_{\text{eff}} = \min(T_{\text{eff}}, 60000)$. It should be noticed that most of the main-sequence lifetime of VMOs is spent at $T_{\text{eff}} > 60000$.

2.2. Effect of rotation

As shown by e.g. Friend & Abbott (1986) and Pauldrach et al. (1986), radiative mass-loss rates are enhanced by rotation by

a factor that depends on the ratio, $v_{\text{rot}}/v_{\text{crit}}$, between the rotational velocity (usually taken at the equator), and the critical or break-up velocity. This latter is defined by the vanishing of the net radial acceleration contributed by the gravitational, radiative, and centrifugal forces.

In our work we apply the analytic recipe presented in Maeder & Meynet (2000, and earlier works of the series referenced therein), where the results of a detailed quantitative analysis of stellar rotation are conveniently synthesised. According to Maeder & Meynet's scheme, the mass-loss rate from a rotating star can be expressed as a function of the purely radiative \dot{M}_{rad} , and the rotational correction factor:

$$\dot{M}(v_{\text{rot}}) = F_{\Omega} \times \dot{M}_{\text{rad}}(v_{\text{rot}} = 0), \quad (4)$$

with the correction factor given by

$$F_{\Omega} = \frac{(1 - \Gamma)^{\frac{1}{\alpha} - 1}}{[1 - (T_{\Omega} + \Gamma)]^{\frac{1}{\alpha} - 1}}, \quad (5)$$

where Γ is the Eddington factor for electron screening opacity, Ω is the angular velocity, ρ_m is the internal mean density, and α is the force multiplier parameter corresponding to the slope of the line strength distribution.

The effect of rotation is contained in the term

$$T_{\Omega} = \frac{\Omega^2}{2\pi G \rho_m} \simeq \frac{4}{9} \frac{v_{\text{rot}}^2}{v_{\text{crit}}^2}, \quad (6)$$

where the break-up velocity is evaluated as

$$v_{\text{crit}} = \left(\frac{2}{3} \frac{GM}{R} \right)^{\frac{1}{2}} \quad (7)$$

with clear meaning of the quantities.

We refer to the classical Ω -limit when the centrifugal acceleration balances the gravitational one, that is when $v_{\text{rot}} = v_{\text{crit}}$ and the effects of radiation can be neglected. This is not the case of VMOs, as they are characterised by large Eddington factors. The so-called $\Omega\Gamma$ -limit applies, instead, when the effects of both radiation and rotation concur to balance the gravitational acceleration. This corresponds mathematically to the divergency of the factor F_{Ω} , that is when the denominator of Eq. (5) vanishes.

It is worth noticing that for $v_{\text{rot}} = v_{\text{crit}}$, the denominator of Eq. (5) becomes $\sim [0.361 - \Gamma]^{\frac{1}{\alpha} - 1}$ and the $\Omega\Gamma$ -limit could be met for values $\Gamma \geq 0.639$, that is for luminosities fainter than the Eddington limit. Viceversa, if $\Gamma > 0.639$, the $\Omega\Gamma$ -limit could be already reached for rotational velocities lower than v_{crit} , that is below the Ω -limit.

If $\Omega\Gamma$ -limit is attained, then Eq. (4) becomes meaningless, and the theory does not indicate any straightforward simple treatment for such critical occurrence. For the sake of simplicity, we handle this circumstance by assuming a constant value for the mass-loss rate, \dot{M}_{crit} , its value being a free parameter to be specified in our calculations.

The evolution of the rotational velocity $v_{\text{rot}} = \Omega(R) \times R$ (where R is the surface radius) is derived under simple assumptions, namely:

- Spherical symmetry

- Rigid-body rotation, $\Omega(r) = \Omega$
- Conservation of the current total angular momentum over any evolutionary time step
- The equations of stellar structures are kept unchanged, i.e. without including any rotational term.

In summary, we proceed as follows. Let us suppose that at a given time t the total angular momentum of the star is

$$\mathcal{L}(\Omega) = \Omega \times \mathcal{J}, \quad (8)$$

where

$$\mathcal{J} = \frac{8\pi}{3} \int_0^R \rho(r) r^4 dr \quad (9)$$

is the moment of inertia of the stellar sphere. All quantities, like the stratification in radial coordinate r , density ρ and surface radius R , are evaluated at t .

If during the evolutionary time step, $\delta t = t' - t$, the star has lost a shell of mass δM , comprised between radii \bar{r} and R , then the total angular momentum at time t' is given:

$$\begin{aligned} \mathcal{L}'(\Omega') &= \Omega' \times \frac{8\pi}{3} \int_0^{R'} \rho'(r') r'^4 dr' \\ &= \mathcal{L}(\Omega) - \Omega \times \frac{8\pi}{3} \int_{\bar{r}}^R \rho(r) r^4 dr \end{aligned} \quad (10)$$

where all primed quantities are now referred to time t' .

In this way we can account for the decrease of the total angular momentum due to mass loss (see Heger & Langer 1998), as well as the effects of possible spinning-up (slowing-down) of rotation due to contraction (expansion) of the star.

The free rotation parameters to be specified before calculating each model are: i) the initial rotational velocity $v_{\text{rot},0}$, and ii), the force multiplier parameter α , and the critical mass loss rate \dot{M}_{crit} at the $\Omega\Gamma$ -limit. In our calculations we adopt $v_{\text{rot},0} = 500 \text{ km s}^{-1}$; $\alpha = 0.1, 0.4$; and $\dot{M}_{\text{crit}} = 10^{-3} M_{\odot} \text{ yr}^{-1}$.

We set α lower than the standard value of $2/3$ valid for hydrogenic ions since, according to Kudritzki (2002), α is found to decrease at decreasing metallicities. We notice that the lower α , the larger the correction factor due to rotation F_{Ω} (see Eq. (5)). However, since our results for the case $\alpha = 0.1$ do not substantially differ from those for $\alpha = 0.4$, we will show and discuss only these latter.

Finally, we choose to set \dot{M}_{crit} of the same order of magnitude as the very large mass-loss rates measured in Luminous Blue Variables (LBV), yellow and blue super-giants (see e.g. Leitherer 1997).

2.3. General characteristics

Let us now first consider the general features that characterise the evolution of zero-metallicity VMOs, and then move to discuss the efficiency of mass loss.

It is well known that in stars originally lacking in CNO elements the (pre-)main sequence gravitational contraction of the central regions may proceed to such an extent that the density and temperature conditions allow the ignition of the triple- α

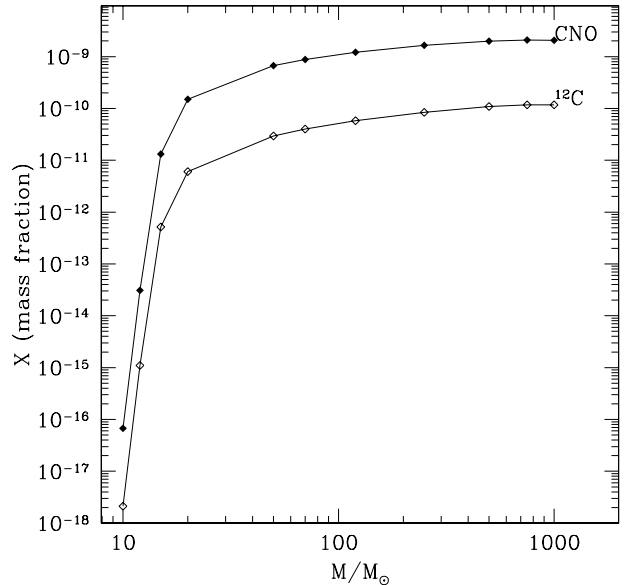


Fig. 1. CNO and ^{12}C central abundances (in mass fraction) when 5% of hydrogen has been burnt in the convective core, as a function of the initial stellar mass

reaction, with consequent activation of the CNO-cycle. In stars with $M \lesssim 20 M_{\odot}$, the first occurrence of the triple- α reaction usually takes place after core H-burning has already started via the p-p reactions, the time delay between the two events reducing at increasing stellar mass. Eventually, in more massive stars, with $M \gtrsim 20 M_{\odot}$, the first synthesis of primary ^{12}C is practically simultaneous with the onset of core H-burning, which proceeds via the CNO cycle since the very initial stages.

This is illustrated in Fig. 1, showing the primary CNO and ^{12}C abundances in the convective core at the beginning of H-burning, as a function of the initial stellar mass. It is worth noticing that $X(\text{CNO}) \sim X(^{14}\text{N})$, because as soon as the triple- α reaction produces some ^{12}C , most of it is immediately burnt into ^{14}N , given the high temperatures at which the CNO-cycle operates. For $M \gtrsim 20 M_{\odot}$, the total $X(\text{CNO})$ has already grown to $\sim 10^{-10} - 10^{-9}$, which guarantees the primary role of the CNO-cycle as nuclear energy source for the star during the whole main sequence phase (see Paper I). The abrupt drop of $X(\text{CNO})$ at lower masses indicates that the full activation of the CNO-cycle is delayed to later stages of H-burning, initially proceeding via the p-p reactions (see also figure 5 in Paper I).

Various model predictions for relevant quantities are presented in Table 1. Let us first consider the nuclear lifetimes of core H- and He-burning (τ_{H} and τ_{He}) as a function of the initial stellar mass. In both cases the trend is initially decreasing at larger masses, until it flattens out towards a nearly constant value of roughly $2 \times 10^6 \text{ yr}$ for τ_{H} and $2 \times 10^5 \text{ yr}$ for τ_{He} , towards the most massive models ($M \gtrsim 500 M_{\odot}$). It is worth briefly recalling the reason for this, with the aid of approximate scaling relations (see Kippenhahn & Weigert 1994), e.g. the definition of the nuclear H-burning lifetime, $\tau_{\text{H}} \propto M/L$, and

Table 1. Evolutionary properties of zero-metallicity VMOs for the adopted mass-loss prescriptions. From left to right the table entries read: the stellar initial mass; the H- and He-lifetimes; the mass of ejecta, carbon and helium cores at central C-ignition; the wind yields of helium, and C,N,O elements. All masses are expressed in M_{\odot} , including the chemical yields. The nuclear lifetimes are given in yr.

M	τ_H	τ_{He}	ΔM_{ej}	M_C	M_{He}	$y(^4He)$	$y(^{12}C)$	$y(^{14}N)$	$y(^{16}O)$
MODELS with $v_{rot} = 0$; $\dot{M} = \dot{M}_{rad}$									
120	2.745E+06	2.557E+05	0.02	50.94	59.95	4.090E-03	6.805E-18	5.536E-16	1.056E-17
250	2.219E+06	2.281E+05	0.19	117.29	132.93	8.655E-07	2.956E-16	1.966E-14	3.595E-16
500	1.943E+06	2.132E+05	11.38	243.00	263.89	1.725E-02	5.251E-12	4.870E-10	8.745E-12
750	1.852E+06	2.111E+05	146.20	343.84	390.89	1.324E+01	4.229E-09	3.983E-07	4.842E-09
1000	1.861E+06	2.153E+05	581.29	346.17	418.67	1.733E+02	4.109E-01	2.057E-05	3.089E-01
MODELS with $v_{rot,0} = 500$ km s⁻¹									
120	2.745E+06	2.550E+05	1.43	50.92	59.99	1.587E-08	3.039E-18	2.478E-16	4.728E-18
250	2.219E+06	2.283E+05	3.35	117.50	132.70	3.853E-06	1.085E-15	8.520E-14	1.587E-15
500	1.941E+06	2.169E+05	20.67	245.22	268.93	5.848E-01	1.767E-10	1.507E-08	2.877E-10
750	1.853E+06	2.092E+05	158.30	343.63	385.81	1.612E+01	5.002E-09	4.682E-07	5.742E-09
1000	1.862E+06	2.155E+05	581.41	344.27	414.40	1.697E+02	1.184E+00	1.733E-05	1.501E+00

the mass-luminosity relation, $L \propto M^{\eta}$, so that $\tau_H \propto M^{1-\eta}$. As the exponent η is typically 3-3.5 (say in the range from about 1 to $100 M_{\odot}$), the nuclear lifetime is expected to decrease at increasing stellar mass. The almost invariance of τ_H seen at very large masses is the result of the growing contribution of radiation to the total pressure, which makes the mass-luminosity relation approach a linear proportionality ($\eta \sim 1$ and $L \propto M$), so that $\tau_H \approx const$.

One common feature of the VMO models is the development of very large convective cores during both the H- and He-burning phase, with a typical fractional extension amounting to 70 – 90 % of the total mass. Moreover, at the exhaustion of hydrogen in the core central convection does not disappear, and the onset of core He-burning immediately follows because of the already high temperatures attained ($\log T \sim 8.2 - 8.3$). This implies that the intermediate phase of H-shell burning is not expected for these stars.

Two examples are illustrated in Figs. 2 and 3, that show the evolution of both convective and burning regions in two models with initial masses of $250 M_{\odot}$ and $1000 M_{\odot}$, for two choices of the mass-loss prescription. From these plots we can already see that new products synthesised by nuclear burnings may be exposed to the stellar surface because of i) the inward penetration of the convective envelope across a chemical profile left by the gradual recession of the convective core, and/or ii) the progressive peeling of the stars due to mass loss. This point will be discussed in more detail in the following sections.

Figure 4 displays the evolutionary tracks in the H-R diagram for the two sets of VMOs, calculated adopting the prescriptions for purely radiative and rotational-radiative mass loss, respectively. In all cases central H-burning is mostly spent at high effective temperatures, regardless the efficiency of mass loss. We can notice that the locus of points describing the onset of core He-burning (practically coincident with the end of core H-burning) bends towards lower T_{eff} at increasing stellar mass. On the other hand, the He-burning phase takes place

in different regions of the H-R diagram, depending on stellar mass and mass loss. Soon after the onset of He-burning, models with $120 M_{\odot} \leq M \leq 750$ are able to reach their Hayashi line, where they remain up to central carbon ignition. The evolution of models with $M = 1000 M_{\odot}$ takes place entirely at high effective temperatures, essentially due significant mass loss. Next section will examine this aspect in mode detail.

Finally, Fig. 8 shows the expected behaviour of the mass of the He- and CO- core at the stage of central carbon ignition, as a function of the initial mass in the domains of massive and very massive stars ($8 M_{\odot} \leq M \leq 1000 M_{\odot}$). The relation is almost linear, without any important effect due to mass loss. Our predictions indicate that the interval $M_{He} = 64$ to $133 M_{\odot}$, which would produce pair-instability supernovae according to Heger & Woosley (2002)'s recent calculations, correspond to stellar progenitors with initial masses $M = 127$ to $252 M_{\odot}$ (see also El Eid et al. 1983, Ober et al. 1983, Bond et al. 1984, Carr et al. 1984).

2.4. Mass-loss efficiency

We will discuss now the efficiency of mass loss in relation to the two driving mechanisms here considered, namely: radiation (Sect. 2.1) and rotation (Sect. 2.2). Stellar ejecta are presented in Table 1.

Models with $\dot{M} = \dot{M}_{rad}$. In general, the purely-radiative mass-loss rates remain quite low during the whole evolution of VMO models with $M < 500 M_{\odot}$. For instance, the $120 M_{\odot}$ model returns only $0.02 M_{\odot}$ to the interstellar medium. In this mass range, the general properties are practically the same ones as those predicted for constant-mass evolution. As reasonable extrapolation we could expect that at lower masses ($< 120 M_{\odot}$, hence lower luminosities), the inefficiency of mass loss should even more marked, which supports the scenario of constant-mass evolution of Pop-III stars discussed in Paper I. Another

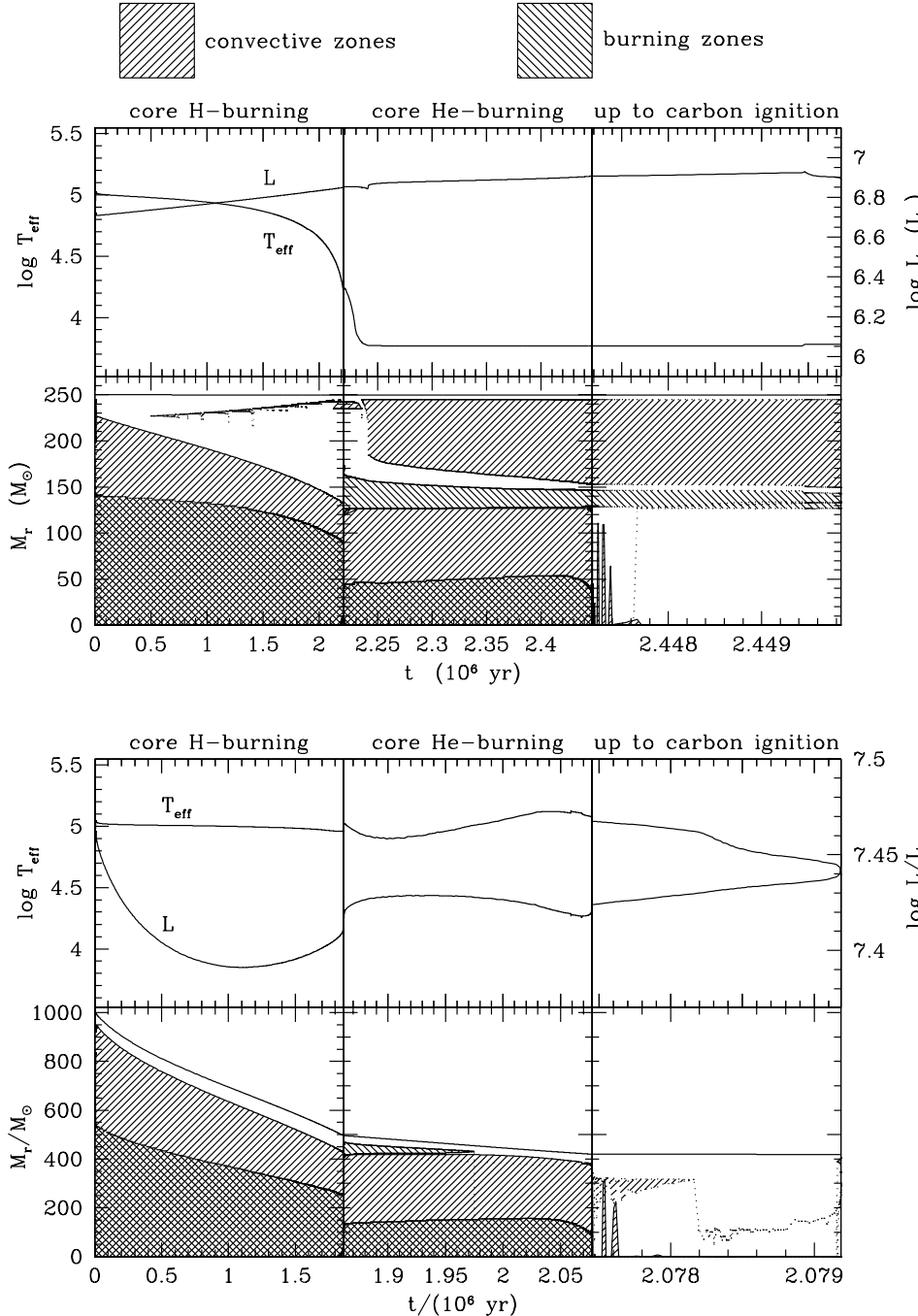


Fig. 2. Evolutionary properties of the $250 M_\odot$ model with the prescription for the purely radiative mass loss. Top panel: Stellar luminosity and effective temperature as a function of time during the major nuclear burnings up to central carbon ignition. Bottom panel: Convective and burning regions (in mass coordinate from the centre to the surface) across the stellar structure. The upper solid line represents the mass coordinate of the stellar surface

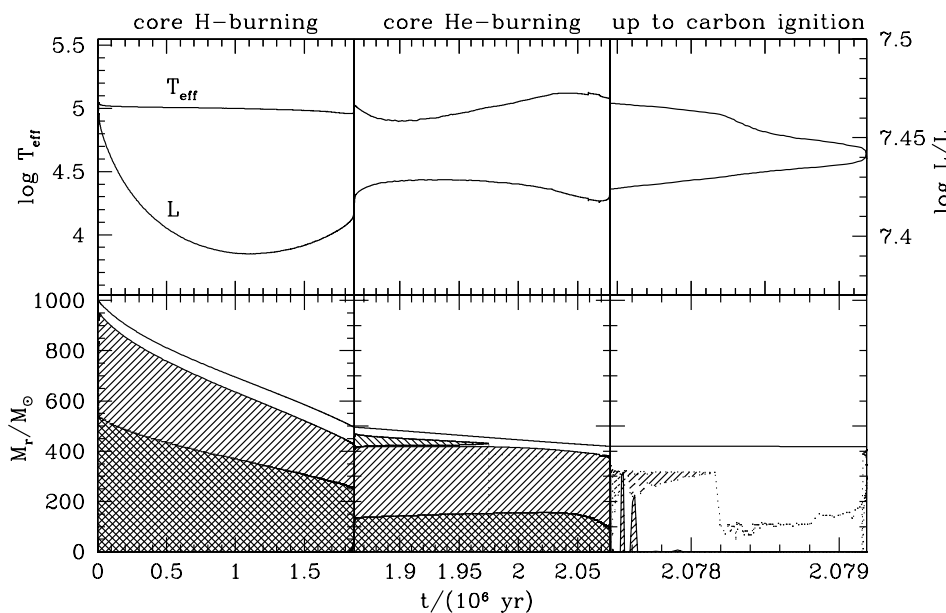


Fig. 3. The same as in Fig. 2, but referring to the evolution of the $1000 M_\odot$ model calculated with the prescription for radiative-rotational mass-loss. The assumed initial rotational velocity is $v_{\text{rot}} = 500 \text{ km s}^{-1}$. An almost identical plot is obtained for the model with the same initial mass, but assuming the purely radiative mass-loss rates

common characteristic of the models with $M = 120 - 500 M_\odot$ is the morphology of the tracks in the H-R diagram, and hence the location of major nuclear burnings. Actually, if the H-burning phase is spent in regions of high effective temperature (typically at $\log T_{\text{eff}} \sim 4.8 - 5.0$), the subsequent He-burning phase takes place far away from there, as the star evolves along its Hayashi line (typically at $\log T_{\text{eff}} \sim 3.7 - 3.8$). Indeed, the tracks of models with $M < 500 M_\odot$ are characterised by quite a large excursion in T_{eff} , that is performed at almost constant luminosity.

Similar considerations on the morphology of the tracks in the H-R diagram apply to the $750 M_\odot$ model as well, though

in this case the efficiency of mass loss is somewhat more significant, the total ejecta amounting to about 20% of the initial mass (see Table 1).

A different behaviour characterises the most massive model here considered, with $M = 1000 M_\odot$. In this case, radiative mass loss is predicted to be strong since the very beginning of the MS phase, due to the combination of large luminosities and effective temperatures. The entire evolution is confined in regions of the H-R diagram of high effective temperatures, and the corresponding stellar ejecta up to the central carbon ignition are considerable, reaching to more than half the initial mass.

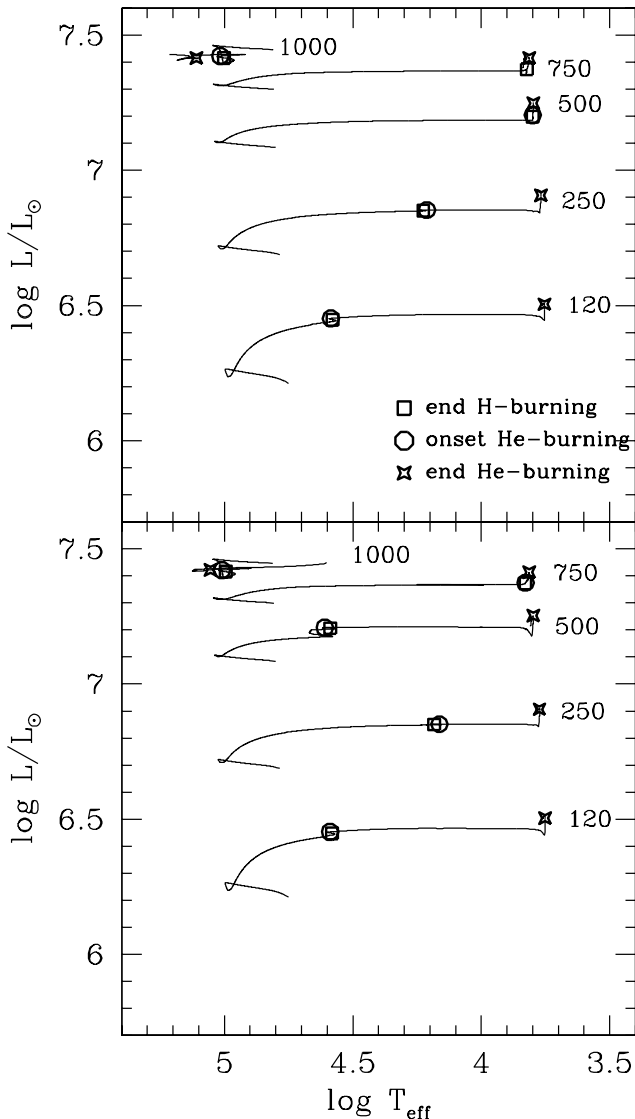


Fig. 4. Zero-metallicity stellar tracks of VMO with initial masses of $120, 250, 500, 750, 1000 M_{\odot}$. The evolution covers the H- and He-burning phases up to ignition of central carbon. **Top panel:** Purely radiative mass-loss prescription; **Bottom panel:** Rotational-radiative mass-loss prescription

The net result is that radiation-driven stellar winds do not produce appreciable mass loss from massive zero-metallicity stars, except for the most massive models, with $M > 750 M_{\odot}$. Our finding supports previous indications in this sense by Kudritzki (2000) and Bromm et al. (2001).

It is worth making a final remark by looking at Fig. 5, which displays the degree of chemical self-pollution at the surface, in terms of CNO abundance, produced by the combined effect of mass loss and convective mixing. As we see in most models the maximum enrichment does not exceed $10^{-9} - 10^{-8}$, that is the critical CNO abundance required in stars with original metal-free composition to fully activate the CNO-cycle as dominant energy source (see Sect. 2.3 and Fig. 1). This occurs when the mass-loss front is only able to penetrate into the chemical pro-

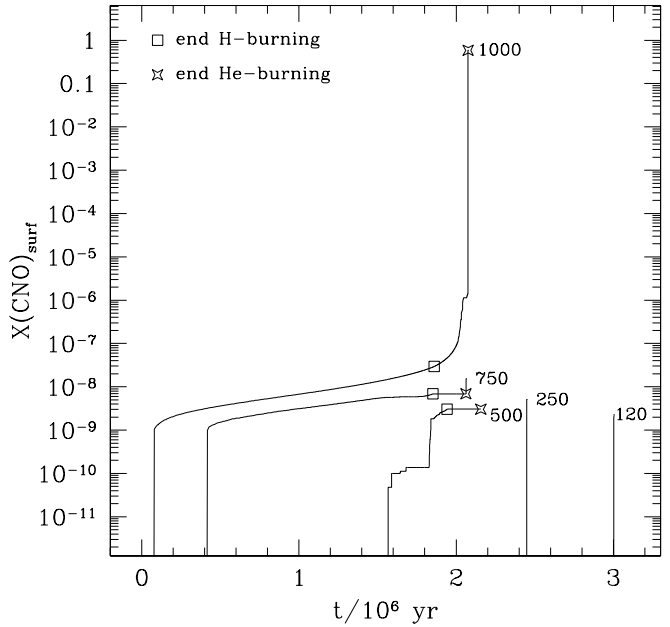


Fig. 5. Surface abundance of CNO elements (in mass fraction) as a function of the evolutionary time, from the ZAMS up to carbon ignition in the core. Curves correspond to different initial masses (as indicated) of VMOs with initial zero metallicity. The radiative mass-loss prescription is applied. Note that in most cases $X(\text{CNO})_{\text{surf}}$ remains lower than Z_{min} assumed in the radiative mass-loss formula (see Sect. 2.1)

file generated by the recession of the convective core during the MS phase, as it is the case of the 500 and $750 M_{\odot}$ models. Models with lower masses, 120 and $250 M_{\odot}$, show comparable self-enrichment, that is however reached after the end of the He-burning phase, not as a consequence of mass loss but because of deep convective dredge-up while on the Hayashi line. It follows that such degree of surface chemical enrichment should not produce enough resonant metal lines in the atmosphere to activate efficient radiation-driven mass-loss.

On the contrary, the most massive $1000 M_{\odot}$ model exhibits a remarkable increase of the CNO abundance during the He-burning phase, due to the progressive reduction of the stellar mass. As shown in Fig. 3 the H-burning shell is extinguished and eventually, close to the exhaustion of central helium, the mass-loss front penetrates into regions previously reached by convective core. Then, significant amounts of carbon and oxygen are exposed at the surface ($X(\text{CNO}) \approx 0.6$). Whenever this circumstance may trigger substantial radiative mass-loss is an interesting point to be considered, and it would deserve a dedicated study in the framework of the radiation-driven-winds theory. Finally, it is worth remarking that an additional chemical pollution of the stellar surface may be caused by rotationally-induced mixing (e.g. Heger & Langer 2000; Meynet & Maeder 2002), which is not taken into account in the present analysis.

Models with $\dot{M} = \dot{M}(v_{\text{rot}})$. The amplification effect on mass loss due to stellar rotation turns out rather limited. As we can see, the evolutionary tracks in bottom panel of Fig. 4 are almost

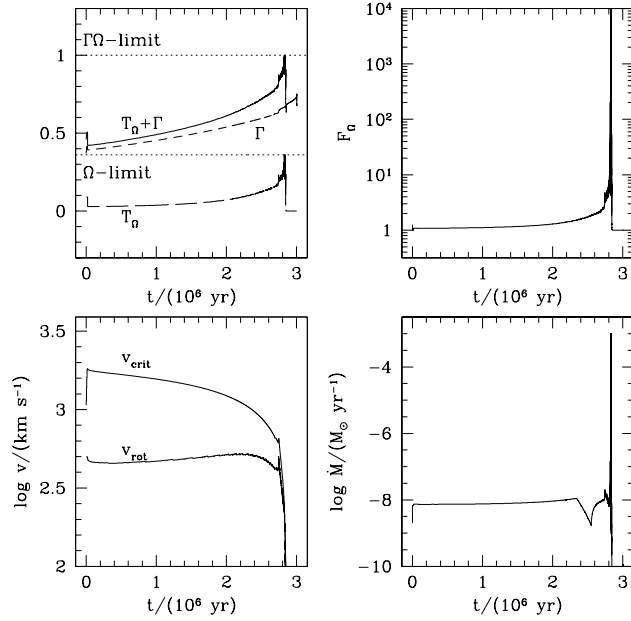


Fig. 6. Evolution of rotational parameters referring to the $120 M_{\odot}$ model, calculated with $V_{\text{rot},0} = 500 \text{ km s}^{-1}$, and $M_{\text{crit}} = 10^{-3} M_{\odot} \text{ yr}^{-1}$. Top-left panel: Relevant terms determining the rotation correction factor given by Eq. (5). The Ω - and $\Omega\Gamma$ -limits are indicated by horizontal lines delimiting the maximum values for T_{Ω} and $T_{\Omega} + \Gamma$, respectively. Top-right panel: Rotation correction factor. Bottom-left panel: Evolution of surface (v_{rot}) and critical (v_{crit}) rotation velocities. Bottom-right panel: mass-loss rate

indistinguishable from those in the top panel. Actually, the total ejecta are larger than those for models with radiative rates, but not such to drastically alter the evolutionary properties just presented.

To better understand the results we refer to Figs. 6 and 7, showing the evolution of rotational parameters and mass-loss rates. In both cases the correction factor F_{Ω} (Eqs. (4) and (5)) keeps close to one during nearly the whole MS phase, so that the mass-loss rate remains quite low ($\sim 10^{-8} M_{\odot} \text{ yr}^{-1}$).

Eventually, during the stages just preceding and following the H-consumption in the core, the $120 M_{\odot}$ model reaches both the Ω - and $\Omega\Gamma$ -limits at the same time. This result is supported by recent analyses of rotating stars at low metallicities. In fact, as discussed by Meynet & Maeder (2002) the approach of the $\Omega\Gamma$ -limit is just favoured in massive and luminous stars at very low- or even zero metallicity. This circumstance should be the consequence of two concurring factors, namely: i) the nearly total conservation of the initial angular momentum during the almost constant-mass evolutionary stages, that would lead to the natural settling of the break-up rotation, hence the Ω -limit; and ii) the large values of the Eddington factor in massive and luminous stars. In practice, both factors favour the divergency of the correction factor given by Eq. (5).

With respect to the former point i), we recall that various analyses (e.g. Heger & Langer 1998, 2000; Meynet & Maeder 2000, Maeder & Meynet 2001) have shown that a massive

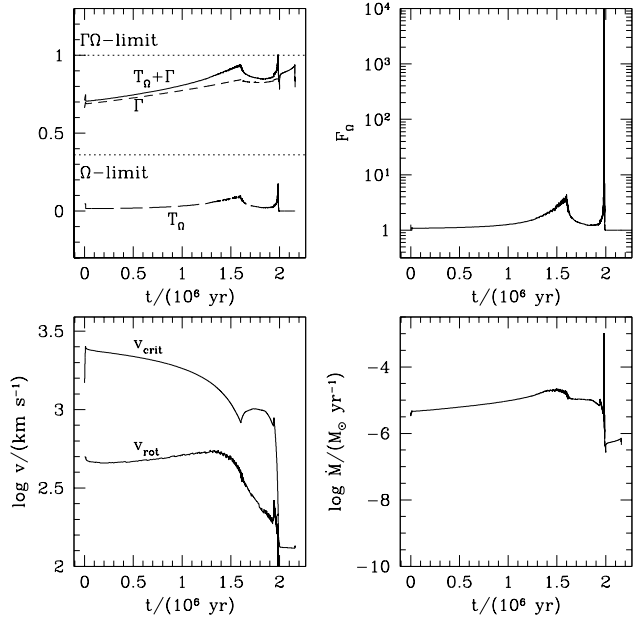


Fig. 7. The same as in Fig. 6, but for the $500 M_{\odot}$ model

star evolving at (nearly) constant mass could approach or even reach the break-up rotation, towards the end of the MS phase (or in a blue-loop off the Hayashi line). In fact during these stages, the progressive stellar contraction would result in increasing surface rotational velocities (the so-called “spin-up phases”). This is exactly what we find in our $120 M_{\odot}$ model displayed in Fig. 6. At this stage the stellar mass is practically the same ($\sim 119.98 M_{\odot}$) as the initial one.

However this critical regime, that we describe by assuming an extremely high mass-loss rate M_{crit} , is maintained only for very short. In fact, the reduction of total angular momentum carried away by the outermost ejected layers, and the increase of the radius due to the subsequent expansion (following the beginning of core He-burning) make rotation to slow down (see bottom-left panel of Fig. 6), with consequent departure from the Ω and $\Omega\Gamma$ -limits.

Then, the star evolves rapidly towards lower effective temperatures onto its Hayashi line, which causes a further drastic decrease of the rotational velocity. The total ejecta with the inclusion of the rotational effect is almost negligible, $\sim 1.5 M_{\odot}$ (see Table 1).

A similar behaviour is found for the $500 M_{\odot}$ model. However, in this case the larger luminosity concurs to lead the star closer to the $\Omega\Gamma$ -limit already during the MS phase. Then, the radiative mass-loss rate is enhanced by a few times (see top-right panel of Fig. 7). Again, the $\Omega\Gamma$ -limit (but not the Ω -limit) is briefly touched during the spin-up phase towards the end of the MS phase, but soon after abandoned because of the loss of angular momentum and the expansion of the star. Compared to the model with the same initial mass but with radiative mass loss, the net effect of rotation is to increase the total ejecta by roughly a factor of two, which still remains very small (see Table 1).

At larger masses ($M = 750, 1000 M_{\odot}$) the effect of rotation turns out even weaker. In fact, for these models the radiation-driven mass loss becomes efficient, which leads to the removal of a significant part of the original angular momentum already during the MS, hence preventing the approaching of the critical Ω and $\Omega - \Gamma$ -limits.

2.5. Cautionary remarks

At this point it is worth making a few cautionary remarks about the assumptions and simplifications adopted in our work to describe the effect of mass loss in primordial massive stars.

As far as the radiative mass-loss is concerned (Sect. 2.1), it should be pointed out that the position $Z = \max(Z_{\min}, Z_{\text{eff}})$ and the treatment for $T_{\text{eff}} > 60000$ K may lead to overestimate the actual mass-loss rates, since for instance the minimum metallicity, $Z_{\min} \sim 10^{-6}$, is typically two orders of magnitude larger than Z_{eff} , (except for the $1000 M_{\odot}$ model). Moreover, the application of the formula for \dot{M}_{rad} to models with $M > 500 M_{\odot}$ requires to extrapolate the predictions above the upper-limit in luminosity (i.e. $\log(L/L_{\odot}) = 7.03$) of the validity domain.

The simplifying assumption at this stage, without calculations for $T_{\text{eff}} > 60000$ K and $\log(L/L_{\odot}) > 7.03$ available, is that the line force parametrisation at higher temperatures and luminosities is still reasonably approximated in this way. New calculations extending the temperature and luminosity domains are certainly needed for the future.

As far as the rotational mass-loss is concerned (Sect. 2.2), we recall that the results are obtained in the ambit of a very simplified description of stellar rotation (mainly due to the assumption of solid-body rotation). It is clear that a strictly correct procedure should consider important processes like meridional circulation, shears, and horizontal turbulence, which would also determine a feed-back on stellar structure (see e.g. Kippenhahn & Thomas 1970; Meynet & Maeder 1997). Among the main related effects, it turns out that the outward transportation of angular momentum from the central regions by meridional circulation would produce a differential rotation. These aspects are not included in the present work.

Rather, our assumption of solid-body rotation would ideally correspond to the case of maximum efficiency of convection and shears in the transport of angular momentum from the inner to the outer regions of the star. In this way even a relatively small loss of material from the surface leads to a substantial loss of the total angular momentum, and consequently to the slow-down of rotation.

On the other hand, in the context of a detailed treatment of rotation – coupled to stellar structure and including also the role of meridional circulation – we may expect that the outward transport of angular momentum is less efficient. In fact, detailed computations accounting for differential rotation (e.g. Meynet & Maeder 2000, 2002) indicate that i) the angular velocity increases progressively with time towards the centre, and ii) the break-up rotation could be reached earlier and maintained for longer periods. Moreover, the possible effect of anisotropic mass loss (Maeder 2002) could further reduce

the loss of angular momentum and lead to earlier break-up. Finally, two additional effects are expected to gain increasing importance at lower metallicity, namely: i) faster core rotation and more efficient rotational mixing (Meynet & Maeder 2002), and ii) possibly larger initial rotational velocities (Maeder et al. 1999).

These considerations lead to the possibility that the combined effects of rotation and mass loss may be somewhat underestimated in our calculations.

It follows that the inclusion of all these aspects might produce different results compared to those presented in this paper. However, since up to now there is no dedicated analysis addressing such issues specifically for Pop-III stars, we believe that our simplified exploration of the effect of rotation on primordial stars should keep its own validity.

3. The stellar yields

If ever formed, massive primordial stars marked the first step in the chemical evolution of the Universe (e.g. Oh et al. 2001; Scannapieco et al. 2002). The efficiency of their contribution to the chemical enrichment of the pristine gas depends essentially on two factors, namely: the individual stellar yields, and the details of the IMF.

As for the former ingredients, predictions of elemental yields are available in Woosley & Weaver (1995) for supernovae II explosions produced by zero-metallicity stars with initial masses in the range $11 - 40 M_{\odot}$, and in Heger & Woosley (2002) for pair-instability supernovae, involving helium core masses in the range $64 - 133 M_{\odot}$ (corresponding to initial stellar masses of $140 - 260 M_{\odot}$ under the hypothesis of constant-mass pre-supernova evolution). According to the latter work, at both lower and larger masses, no explosive nucleosynthesis should be injected into the primordial interstellar medium (ISM) but, rather, trapped into black holes. For past works on pair-instability supernovae the reader could refer to El Eid et al. (1983), Ober et al. (1983), Bond et al. (1984), Carr et al. (1984).

In their evolutionary calculations at initial zero metallicity Woosley & Weaver (1995) and Heger & Woosley (2002) did not consider any mass loss during the hydrostatic phases (except for that driven by pair-instability pulsation). Past calculations of the wind contributions from VMOs can be found in the works by El Eid et al. (1982), Klapp (1983, 1984), and more recently Portinari et al. (1998). These latter estimates are based on the results of semi-analytic stellar models developed by Bond et al. (1984). Our predictions of the wind ejecta from Pop-III VMOs are given in Table 1 that presents, for each model with initial mass M , the net wind yields (in M_{\odot}) of ${}^4\text{He}$, ${}^{12}\text{C}$, ${}^{14}\text{N}$, and ${}^{16}\text{O}$, the total ejecta ΔM_{ej} , and the masses of the He-core (M_{He}) and C-core (M_{C}) at the ignition of central carbon. For the sake of completeness, the results are grouped on the basis of the adopted mass-loss prescriptions, namely: purely-radiative mass loss, and radiative-rotational mass-loss. However, the differences between the two sets of yields are quite small (see Sect. 2.4).

It turns out that the wind yields ejected by VMOs are practically negligible for all masses, except for the two most mas-

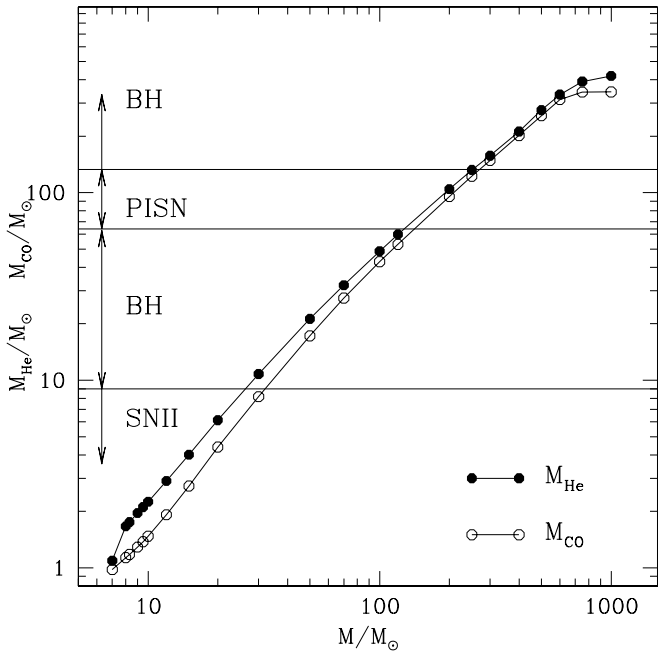


Fig. 8. Masses of the He- and CO- cores at the onset of carbon ignition in the core, as a function of the stellar initial mass. They correspond to evolutionary calculations at constant mass for $M \leq 100 M_{\odot}$ (Marigo et al. 2001), and with radiation-driven mass loss for VMOs for $120 M_{\odot} \leq M \leq 1000 M_{\odot}$. Relevant ranges of M_{He} are marked and labelled – following Woosley & Weaver (1995); Heger & Woosley (2002) – as a function of the final fate of the stellar progenitor, namely: i) black hole (BH) collapse without explosion ($M_{\text{He}} > 133 M_{\odot}$); ii) pair-instability supernovae (PISN, $64 M_{\odot} \leq M_{\text{He}} \leq 133 M_{\odot}$); iii) black hole (BH) collapse after the final explosion ($9 M_{\odot} \leq M_{\text{He}} < 64 M_{\odot}$) iv) SNII explosion with stellar remnant ($1.3 M_{\odot} \leq M_{\text{He}} < 9 M_{\odot}$)

sive models here considered, with $M = 750, 1000 M_{\odot}$. For instance, the $1000 M_{\odot}$ model with $v_{\text{rot},0} = 500 \text{ km s}^{-1}$ ejects about 17% of its initial mass as newly synthesized helium, and $1 - 1.5 M_{\odot}$ in form of carbon and oxygen. In this particular case (see Fig. 3), during the MS phase the mass-loss front eats up the chemical profile left by the receding convective core and the wind ejecta, returned to the ISM, are mainly enriched in ${}^4\text{He}$ and ${}^{14}\text{N}$. Then, during the subsequent He-burning phase, the deep peeling keeps going on to such an extent that, after the ejection of the entire hydrogenic envelope (when the abundance of central helium is ~ 0.03), the mass-loss front extends beyond the extinguished H-burning shell, eventually exposing to the surface the nuclear products of partial core He-burning, mainly ${}^{12}\text{C}$ and ${}^{16}\text{O}$. However, the net yields of these elements are not extremely large, given the short evolutionary time-scales involved from that stage up to the central carbon ignition (i.e. the end of calculations).

3.1. Chemical enrichment and primordial $\Delta Y/\Delta Z$

The extent of helium enrichment, ΔY , supplied by Pop-III stars in the very early stages of cosmic chemical evolution, is a potentially important issue for its possible cosmological implications. For instance, the age of Globular Clusters (GC), as inferred from observations, depends sensitively on the assumed initial helium abundance Y_{p} , which is commonly thought to sample the primordial Big Bang nucleosynthesis (BBN). Typically, an increment of the fractional mass abundance $\Delta Y_{\text{p}} = 0.02$ would produce an age decrement of roughly 15%, that is of the order of 2 Gyr within the range $10 - 15$ Gyr (see e.g. Shi 1995). Moreover, the relative enrichment of helium with respect to that of metals – the so-called $\Delta Y/\Delta Z$ – produced by Pop-III stars, could largely differ from that derived – both theoretically and observationally – at non-zero metallicities, so that the usually adopted linear extrapolation down to $Z = 0$ to infer the primordial helium abundance may lead to misleading results.

Another cosmological issue is related to the nature itself of the dark matter present in galactic haloes and clusters. The standard hot BBN predicts an upper limit to the baryonic density parameter, $\Omega_{\text{BBN}} < 0.06 h_{50}^{-2}$ (where h_{50} is the Hubble constant in units of $50 \text{ km s}^{-1} \text{ Mpc}^{-1}$; see e.g. Kernan & Krauss 1994), that is already lower than the present density parameter inferred from dynamical estimates of virialized systems, $\Omega_{\text{dyn}} \sim 0.1 - 0.2$ (e.g. Dekel 1994). This discrepancy could be solved – without losing, at the same time, the consistency between BBN predictions and the observed elemental abundances (like those of deuterium and lithium) at the lowest metallicities – by invoking that the bulk of dark matter is in a non-baryonic, still unknown, form. This is the commonly accepted picture.

An alternative scenario might arise from the assumption that, instead, dark matter was made of baryons, e.g. in form of the remnants of pre-galactic stars. Were this the case, the immediate dramatic consequence would be that we should abandon the standard BBN, and ascribe the first synthesis of light elements, like deuterium and helium, as well as the photon microwave background to another source. Bond et al. (1983) and Carr et al. (1984) pointed at Pop-III very massive stars as potential candidates, and investigated the extreme possibility that these stars synthesised a substantial fraction, or even the totality, of primordial helium. In that case, a related constraint is that the accompanying metal enrichment does not exceed the upper limits set e.g. by the metallicities measured in Population I and II stars.

In order to derive an updated picture of the aforementioned aspects on the basis of the present results, we have calculated the helium and metal enrichments produced by a population of (very) massive zero-metallicity stars, with $10 M_{\odot} \leq M \leq 8 \times 10^4 M_{\odot}$. No other sources are considered, such as the wind yields from low- and intermediate-mass stars in the Asymptotic Giant Branch (AGB) phase (with $0.7 M_{\odot} \lesssim M \lesssim 8 M_{\odot}$). In other words, we assume that the primordial initial mass function favoured the formation of massive objects, a hypothesis that is supported by current models of primeval cloud fragmentation (e.g. Bromm et al. 1999, 2002; Nakamura & Umemura 2001; Abel et al. 2000). The choice of $8 \times 10^4 M_{\odot}$ as maxi-

mum mass value is motivated by the indications that above this limit stars are not expected to experience static nuclear burnings because of post-Newtonian instabilities, and the chemical enrichment from these super-massive objects should be small (Fricke 1973, Ober 1979; see also Ober et al. 1983).

In summary, we account for the chemical contributions from three groups of stars, namely: i) massive objects (MOs) with masses of $12\text{--}40 M_{\odot}$, that experience no steady mass loss and undergo SN II explosions; and ii) VMOs with initial masses of $120\text{--}260 M_{\odot}$, that may experience mass loss via stellar winds and pair-instability SN explosions; and iii) VMOs with initial masses of $260\text{--}8 \times 10^4 M_{\odot}$ that may suffer mass loss during the hydrostatic phases, before collapsing into black holes. As for the MOs, we adopt the supernova yields at $Z = 0$ calculated by Woosley & Weaver (1995). For the VMOs with initial masses of $120\text{--}1000 M_{\odot}$, we combine our estimated wind contributions with the supernova yields (if non zero) by Heger & Woosley (2002). The matching between the wind and SN yields is performed as a function of the helium core mass as tabulated in Heger & Woosley (2002). Finally, for stars more massive than $1000 M_{\odot}$, we adopt simple analytical prescriptions to estimate the helium and metal yields ejected by steady mass loss over the hydrostatic hydrogen-burning phase. Following Bond et al. (1984) we assume the maximum possible helium yield, which is expressed as a function of the initial electron molecular weight (their equation 27). The corresponding metal enrichment is obtained by multiplying an average CNO abundance (newly synthesised during the core hydrogen-burning, typically $\langle X(\text{CNO}) \rangle \approx 10^{-9}\text{--}10^{-8}$, see Sect. 2.1) by the amount of ejected mass (derived by equating their equations 24 and 27). With our choices for the primordial hydrogen and helium abundances ($X_0 = 0.77$, and $Y_0 = 0.23$ respectively), we obtain the fractional yields – normalised to the initial stellar mass – for objects with $M > 1000 M_{\odot}$:

$$\begin{aligned} y(\text{He})/M &= 0.17 \\ y(\text{CNO})/M &= 0.435 \times \langle X(\text{CNO}) \rangle \end{aligned}$$

In our calculations we assume $\langle X(\text{CNO}) \rangle = 10^{-8}$.

In a similar manner as in Ober et al. (1983), a very simple chemical model is assumed: stars formed in a single burst from a primeval cloud, that is assimilated to a closed box system, chemical enrichment is considered instantaneous with the burst and homogenised throughout the gas.

The basic free parameters that define our model are: the fraction of the primordial cloud, with original mass M_0 , globally consumed in the burst of star formation, $f_s = M_s/M_0$, and the details of primordial IMF (in number of stars per unit mass interval):

$$\phi(M) = \mathcal{A}M^{-x} \quad \text{for } M_{\text{low}} \leq M \leq M_{\text{up}}, \quad (11)$$

where x is the slope of the assumed power law ($x = 2.35$ describes the classical Salpeter relation); M_{low} , M_{up} correspond to the minimum and maximum values of the initial stellar mass, respectively.

The quantity \mathcal{A} in Eq. (11) must satisfy the condition

$$\begin{aligned} M_s &= \int_{M_{\text{low}}}^{M_{\text{up}}} M\phi(M)dM = \mathcal{A} \int_{M_{\text{low}}}^{M_{\text{up}}} M^{1-x}dM \\ &= \mathcal{A} \times \xi \end{aligned} \quad (12)$$

Denoting with $\Delta^W(M)$, $\Delta^{\text{SN}}(M)$ the masses of the ejecta contributed by a star with initial mass M via stellar winds and supernova explosions, respectively, then the final mass of the cloud, left in form of gas after the burst of star formation, is

$$\begin{aligned} M_f &= M_0 - M_s + \mathcal{A} \int_{M_{\text{low}}}^{M_{\text{up}}} [\Delta^W(M) + \Delta^{\text{SN}}(M)]M^{-x}dM \\ &= M_0 - M_s + \mathcal{A} \times \mathcal{R} \end{aligned} \quad (13)$$

Analogously, the final mass of the cloud in form of any given element j can be derived from

$$\begin{aligned} M_j &= (M_0 - M_s)X_{j,0} + \mathcal{A} \int_{M_{\text{low}}}^{M_{\text{up}}} \{y_j^W(M) + y_j^{\text{SN}}(M) \\ &\quad + [\Delta^W(M) + \Delta^{\text{SN}}(M)]X_{j,0}\}M^{-x}dM \\ &= (M_0 - M_s)X_{j,0} + \mathcal{A} \times \mathcal{R}_j \end{aligned} \quad (14)$$

where $X_{j,0}$ denotes the initial abundance of the element j , $y_j^W(M)$ and $y_j^{\text{SN}}(M)$ are the corresponding yields (in mass units) due to stellar winds and SN explosion, respectively. In Eqs. (13) and (14) the quantities \mathcal{R} and \mathcal{R}_j are a measure of the integrated efficiency of the primordial stellar population in terms of restitution to the ISM of gas, and elemental abundances, respectively.

Finally, after simple algebraic passages, we estimate the fractional abundance (by mass) of the element j in the gas resulting from the chemical enrichment by Pop-III stars:

$$\Delta X_j = X_j - X_{j,0} = \frac{M_j}{M_f} - X_{j,0} = \frac{f_s(\mathcal{R}_j - \mathcal{R}X_{j,0})}{(1 - f_s)\xi + f_s\mathcal{R}} \quad (15)$$

We apply the above formula to derive the global enrichment of helium, ΔY , and metals ΔZ produced by a Pop-III burst of star formation. We set $Y_0 = 0.23$ and $Z_0 = 0$. The results can be analysed as a function of the efficiency of star formation (expressed by the parameter f_s), and different choices of the IMF. Figures 9 and 10 show few illustrative examples, that bracket the widest variability range of the results for different combinations of the model parameters. In practice we consider five cases, namely: i)–ii) classical Salpeter IMF (with $x = 2.35$) over the mass intervals $10\text{--}1000 M_{\odot}$ and $10\text{--}8 \times 10^4 M_{\odot}$; iii)–iv) Salpeter-like but flatter IMF (with $x = 1.5$) with the inclusion of VMOs only, over the mass intervals $120\text{--}1000 M_{\odot}$ and $120\text{--}8 \times 10^4 M_{\odot}$; and v) the same as the previous cases but for a very narrow mass range at about $1000 M_{\odot}$.

As for the helium enrichment, illustrated in Fig. 9, we can make the following remarks. In all cases, ΔY increases with the efficiency of star formation such that an amount of helium, comparable with the primordial value predicted by standard BBN, could be produced by Pop-III massive stars if $f_s \sim 1$. This finding is in agreement with the results by Bond et al. (1983). However, leaving aside this extreme and unlikely condition, we notice in Fig. 9 that, at any f_s , the largest contributions come under the assumption of an extremely top-heavy IMF either narrowly peaked at $\sim 1000 M_{\odot}$ (short-dashed line), or including the contribution of super-massive objects up to $8 \times 10^4 M_{\odot}$ (long-dashed line).

In these particular cases a helium enrichment already of the order of $\Delta Y \sim 0.01$, hence able to affect the age determination

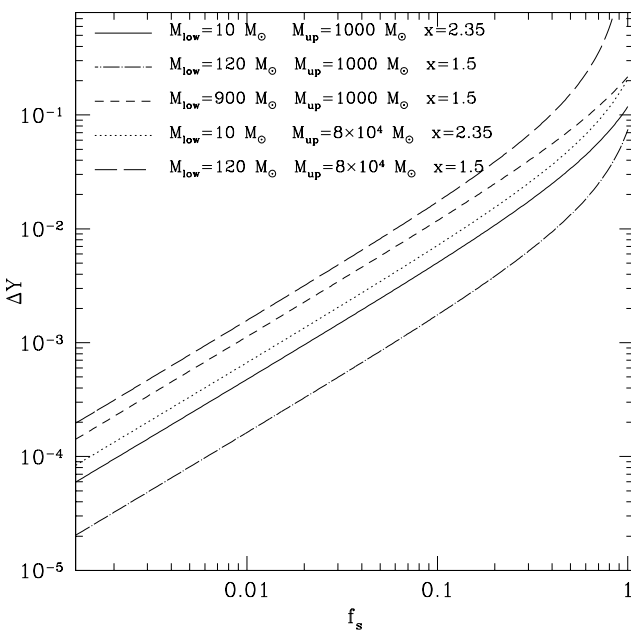


Fig. 9. Helium enrichment produced by a primordial simple stellar population as a function of the star formation efficiency, according to different prescriptions, as indicated

of GCs, may be attained for $f_s \approx 0.05 - 0.1$. Interestingly, these are typical values of the star formation efficiency as indicated by hydrodynamical models of structure and galaxy formation (e.g. Abel et al. 1999; Kawata 2001; Chiosi & Carraro 2002),

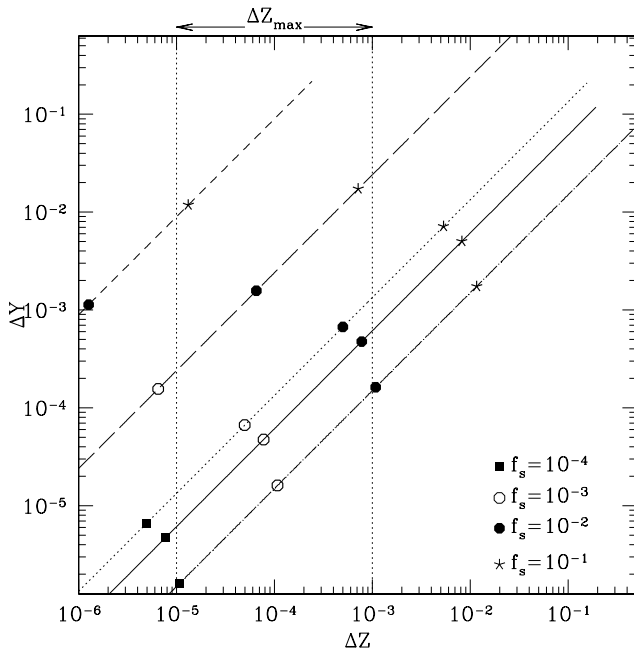


Fig. 10. Helium enrichment as a function of metal production. The illustrated cases refer to the same prescriptions (and corresponding line styles) as described in Fig. 9. Selected values of the star formation efficiency parameter, f_s , are marked along the curves

and chemical evolution of the intra-cluster medium (Moretti et al. 2002). Although the efficiency of star formation somewhat depends on the assumed IMF regulating the energy input from supernova explosions, stellar winds, UV flux etc, in reality it is the result of a delicate balance among several concurring physical processes such as the energy input above, cooling of gas by radiative mechanisms, and dynamical conditions establishing when a gas particle of the hydrodynamical models is able to form stars, so that the role of the IMF is of minor relevance (see Chiosi & Carraro (2002) for a detailed discussion of these topics). An efficiency of star formation $f_s \approx 0.05 - 0.1$ is a sort of general rule. For the Salpeter case (solid and dotted lines in Fig. 9), $\Delta Y \sim 0.01$ could be reached if assuming a larger star formation efficiency, $f_s \approx 0.1 - 0.2$.

However, before drawing any conclusion, it is necessary to perform another important check, related to the concomitant production of heavy metals, ΔZ . In fact, Pop-III metal enrichment should be constrained not to exceed observed upper limits, such as the lowest metallicities measured in Population-II Halo stars, or alternatively the metallicities measured in high-redshift, possibly little evolved, environments like the Lyman- α systems.

From spectroscopic analyses of Pop-II stars we can reasonably take $Z \approx 10^{-5}$ as representative upper limit (see e.g. Norris et al. 1996). As for the high-redshift information the situation is more complex as reviewed by Pettini (1999, 2000). At redshift $z \sim 3$, the estimated metallicity goes from $\sim 0.3 - 0.1 Z_\odot$ in Lyman break galaxies (LBG), $\sim 0.1 - 0.01 Z_\odot$ in Damped Lyman- α systems (DLA), down to $0.01 - 0.001 Z_\odot$ in Lyman- α forests. The metallicity values measured in LBGs and DLAs are relatively high and comparable with the metallicities measured in today's Pop-I and Pop-II stars, so that these systems are likely to have already experienced significant chemical evolution. More plausibly, low-density Lyman- α forests may exhibit, instead, the genuine nucleosynthetic signature of Pop-III stars.

Putting together all these pieces of information, in the present discussion we assume that the maximum allowed metal enrichment should be confined within $10^{-5} \lesssim \Delta Z_{\max} \lesssim 10^{-3}$.

From inspecting Fig. 10, it turns out that for the Salpeter case (solid and dotted lines) the permitted interval of ΔZ_{\max} corresponds to a minor helium enrichment $10^{-5} \lesssim \Delta Y \lesssim \text{few } 10^{-3}$, which is consistent with a quite low star formation efficiency, in the range $10^{-4} \lesssim f_s < 10^{-2}$. This result agrees with previous findings by Ober et al. (1983), and Abia et al. (2001).

On the other hand, in the case of the IMF peaked at $M \sim 1000 M_\odot$ (short-dashed line), ΔZ_{\max} implies a significant helium enrichment, $\Delta Y > 0.01$, and a much larger efficiency of star formation, $f_s > 0.1$. An intermediate situation applies to the case of the extremely top-heavy IMF extending up to supermassive objects (long-dashed line). However, it is worth noticing that under the hypothesis that the first single burst of star formation produced just VMOs with $M \sim 1000 M_\odot$ or supermassive objects, the primordial gas would have been enriched only with CNO elements (and possibly some α -elements),

without any contribution in heavier metals, like the iron-group elements.

Finally, we remark that the helium-to-metal enrichment, $\Delta Y/\Delta Z$, is independent of the star formation efficiency, but is affected by the individual stellar yields and the IMF features. According to our calculations, the two lower curves of Fig. 10 correspond to a $\Delta Y/\Delta Z \sim 0.15 - 0.6$, respectively. These values are quite low compared to recent observational determinations based on HII regions and predictions of chemical evolution models, e.g. $\Delta Y/\Delta Z = 1.9 \pm 0.5$ can be considered a representative value following Peimbert & Peimbert (2001). On the other hand, the highest curve is described by a huge helium-to-metal-enrichment ratio, $\Delta Y/\Delta Z \approx 900$, because of the exceedingly-large helium stellar yield compared to that in the form of CNO elements.

It is clear that this is an extreme situation and large room is allowed for intermediate results in between the case of the Salpeter IMF and that of a IMF peaked at very large masses. Ours is meant as an explorative test indicating that if the primordial IMF was quite different from the classical one, the primordial chemical enrichment may have followed a different path from that one expected under standard prescriptions.

4. Concluding remarks

In this work we have discussed the evolutionary properties of zero-metallicity very massive objects ($120 M_{\odot} \leq M \leq 1000 M_{\odot}$), on the basis of new calculations that extend the work presented in Paper I. Stellar isochrones (see Appendix A) for ages from 16 Gyr down to 10^4 yr are available at the web-address <http://pleiadi.pd.astro.it>.

In the attempt to estimate the possible effects produced by stellar winds from primordial VMOs, we adopt recent formalisms that describe the role of radiation pressure and stellar rotation as mass-loss driving factors. The emerging picture is the following:

- At extremely low metallicity ($Z \approx 10^{-6}$), the mechanism of line-radiation transfer should be scarcely efficient, except for very large masses, say $\gtrsim 750 M_{\odot}$. We also find that, as long as the mass loss front penetrates into the chemical profile left by the convective core during the H-burning phase, the maximum CNO abundance exposed at the surface does not exceed $\approx 10^{-9} - 10^{-8}$, which are typical values required by the CNO-cycle operating in stars with original metal-free composition. Such degree of chemical self-pollution is also too low to trigger efficient radiation-driven winds from zero-metallicity massive stars. Instead, much larger surface enrichment may be attained whenever the nuclear products of He-burning, like carbon and oxygen – potentially able to produce large mass-loss rates – were brought up to the surface by either the penetrating mass-loss front, or some dredge-up process. In our computations this occurs only for the $1000 M_{\odot}$ model.
- Our calculations also indicate that rotating very massive stars may actually reach the critical condition defined as the $\Omega\Gamma$ -limit, which should be likely accompanied by large mass-ejection rates (here taken as large as $\dot{M}_{\text{crit}} = 10^{-3}$

yr^{-1}). However, the net impact on mass loss should be quite limited, given the extremely short time during which these critical regimes can be maintained. To this respect, we remind these results are obtained in the context of a simplified description of stellar rotation, and the reader should consider the remarks expressed in Sect. 2.5.

- Finally we recall that, according to a recent analysis by Baraffe et al. (2001), another possible mass-loss driving mechanism, namely the pulsation instability – usually at work in VMO models with “normal” chemical composition – has been found of modest potential efficiency at zero metallicity, at least for masses $M \lesssim 500 M_{\odot}$.

By combining the supernova yields available in the literature with our predicted wind contributions, we also evaluate, in a simple way, the chemical enrichment produced by a primeval population of (very) massive stars. It is found that a significant helium enrichment, $\Delta Y \sim 0.01$, may be reached by assuming that the primordial conditions in the Universe were such that only very massive stars could form, with typical masses of $\approx 1000 M_{\odot}$, or extending into the super-massive domain (up to $\approx 10^5 M_{\odot}$).

In the former case the implied efficiency of gas-to-star conversion should be of the order of 10%, and the first metal enrichment should be in the form of CNO elements (no iron-group elements). On the other side, under the assumption of the standard Salpeter IMF, the resulting ΔY is indeed negligible over the maximum allowed enrichment in metals, $10^{-5} \lesssim \Delta Z_{\text{max}} \lesssim 10^{-3}$. The corresponding star formation efficiency should be also be quite small, $\approx 0.01 - 0.1\%$.

In any case, as already pointed out long ago by Bond et al. (1983) and Carr (1994), the interesting possibility arises that the first generation of stars could mask the true (somewhat lower) primordial abundance of helium as predicted by the standard Big Bang Nucleosynthesis (e.g. Olive et al. 1997). The question and its implications have been recently addressed by Salvaterra & Ferrara (2002) on the base of the present results.

Appendix A: Isochrones

Basing on the set of evolutionary tracks for VMOs presented in this work, isochrones for very young ages, from $\log t/\text{yr} = 6.6$ down to 4.0, have been constructed. In this way we complement the set of isochrones for zero-metallicity stars already presented in Paper I. In fact, for ages $\log t/\text{yr} < 6.6$ the turn-off point corresponds to stars with $M < 100 M_{\odot}$, which defines the maximum initial stellar mass in the former set of tracks.

An example of the extended isochrones in the H-R diagram is illustrated in Fig. A.1. For ages $2 \times 10^6 \lesssim t/\text{yr} \lesssim 10^8$ the termination point marks the stage of central carbon ignition.

Complete tables with the isochrones can be obtained upon request to the authors, or through the WWW site <http://pleiadi.pd.astro.it>. They cover the complete age range from about 10^4 yr to 16 Gyr ($4.0 \leq \log(t/\text{yr}) \leq 10.25$). Isochrones are provided at $\Delta \log t = 0.05$ intervals. We refer to Paper I (appendix B) and the quoted web-site for all the details

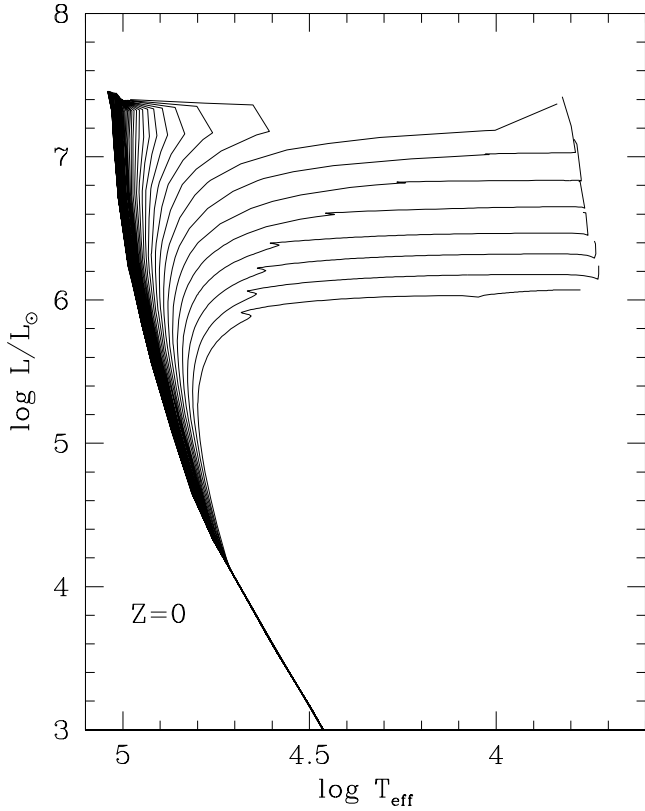


Fig. A.1. Theoretical isochrones in the HR diagram for the initial composition [$Z = 0, Y = 0.23$]. Age ranges from $\log(t/\text{yr}) = 4.0$ to 6.6 , at equally-spaced intervals of $\Delta \log t = 0.05$. In all isochrones, the main sequence extends down to $0.7 M_\odot$ ($\log L/L_\odot \sim -0.5$)

concerning the description of the table format and layout, as well as the sources for magnitude and colour transformations.

Acknowledgements. We are grateful to Léo Girardi for his help in the construction of stellar isochrones; N. Langer, J. Puls, and N.J. Shaviv for useful advice in the matter of stellar winds and stellar rotation. We also thank the referee, D. Schaefer, for many important remarks that much improved the final version of the paper. P.M. and C.C. acknowledge financial support from the Italian Ministry of Education, University and Research (MIUR).

References

Abbott D.C., 1992a, *ApJ* 259, 282

Abbott D.C., 1982b, in *Wolf Rayet Stars: Observations, Physics, Evolution*, ed. C. de Loore & A. J. Willis, p. 185, Dordrecht: Reidel

Abel T., Bryan G. L., & Norman M. L. 2000, *ApJ*, 540, 39

Abel T., Anninos P., Norman M.L., & Zhang Y. 1998, *ApJ*, 508, 518

Abia C., Domínguez I., Straniero O. et al. 2001, *ApJ*, 557, 126

Baraffe I., Heger A., & Woosley S.E. 2001, *ApJ*, 550, 890

Barlow M.J., & Cohen M. 1977, *ApJ*, 213, 737

Bond J.R., Arnett W.D., & Carr B.J. 1984, *ApJ*, 280, 825

Bond J.R., Carr B.J., & Arnett W.D. 1983, *Nature*, 304, 514

Bressan A., Bertelli G., & Chiosi C. 1981, *A&A*, 102, 25

Bromm V., Coppi P. S., & Larson R. B. 1999, *ApJ*, 527, L5

Bromm V., Kudritzki R.P., & Loeb A. 2001, *ApJ*, 552, 464

Bromm V., Coppi P. S., & Larson R. B. 2002, *ApJ*, 564, 23

Carr B. J. 1994, *ARA&A*, 39, 249

Carr B.J., Bond J.R., & Arnett W.D. 1984, *ApJ*, 277, 445

Carr B.J., Bond J.R., & Arnett W.D. 1983, *Nat.*, 340, 514

Castor J.I., Abbott D.C., & Klein R.I. 1975, *ApJ*, 195, 157

Chiosi C. 1981, *A&A*, 93, 163

Chiosi C., & Carraro G. 2002, *MNRAS*, 335, 335

Dekel A. 1994, *ARA&A*, 32

Fricke K.J. 1973, *ApJ*, 183, 941

Friend D.B., & Abbott, D.C. 1986, *ApJ*, 311, 701

Heger A., & Woosley S.E. 2002, *ApJ*, 567, 532

Heger A., & Langer N. 2000, *ApJ*, 544, 1061

Heger A., & Langer N. 1998, *A&A*, 334, 210

Kawata D. 2001, *ApJ*, 558, 598

Kernan P.J., & Krauss L.M. 1994, *Phys. Lett. Rev.*, 72, 3309

Kippenhahn R., & Weigert A. 1994, in *Stellar Structure and Evolution*, Springer-Verlag., p. 207

Kippenhahn R., & Thomas H.-C. 1970, in *Stellar Rotation*, IAU Symp. 4, ed. A. Slettebak, Gordon and Breach Science Publishers, p. 20

Klapp J. 1984, *Astrophys. Space Sci.*, 106, 215

Klapp J. 1983, *Astrophys. Space Sci.*, 93, 313

Kudritzki R.P. 2002, *ApJ*, 577, 389

Kudritzki R.P. 2000, in *The First Stars, ESO Astrophysics Symposia*, ed. A. Weiss, T. Abel, & V. Hill (Berlin: Springer), 127

Kudritzki R.P. 1988, in *Radiation in Moving Gaseous Media*, 18th Advanced Course of the Swiss Society of Astrophysics and Astronomy (Saas-Fee Courses), ed. Y. Chmielewski & T. Lanz, pages 1 - 192

Kudritzki R.P. 1998, in *Stellar Astrophysics for the Local Group, VIII Canary Islands Winter School for Astrophysics*, eds. Aparicio A., Herrero A., Sánchez F., Cambridge University Press, p. 149

Kudritzki R.P., & Puls J. 2000, *ARA&A*, 38, 613

Kudritzki R.P., Mendez, R.H., & Feldmeier, J.J. et al. 2000, *ApJ*, 536, 19

Kudritzki R.P., Pauldrach A.W.A., & Puls J. 1987, *A&A*, 173, 293

Leitherer C. 1997, in *Luminous Blue Variables: Massive Stars in Transition*, ASP Conference Series, 120, eds. Nota A., Lamers H., p.58

Leitherer C., Robert C., & Drissen L. 1992, *ApJ*, 410, 596

Lucy L.B., & Solomon P.M. 1970, *ApJ*, 159, 879

Maeder A. 2002, *A&A*, 392, 575

Maeder A., & Meynet G. 2001, *A&A*, 373, 555

Maeder A., & Meynet G. 2000, *A&A*, 361, 159

Maeder A., Grebel E.K., & Mermilliod J.-C. 1999, *A&A*, 346, 459

Maeder A., & Meynet G. 1997, *A&A*, 321, 465

Meynet G., & Maeder A. 2002, *A&A*, 390, 561

Meynet G., & Maeder A. 2000, *A&A*, 361, 101

Marigo P., Girardi L., Chiosi C., & Wood P.R. 2001, *A&A*, 371, 152 (Paper I)

Moretti A., Portinari L., & Chiosi C. 2002, *A&A* submitted

Ober W.W., El Eid M.F., & Fricke K.J. 1983, *A&A*, 119, 61

Ober W.W. 1979, in *Les Houches XXXII-Physical Cosmology*, eds. Balian et al., North-Holland, Amsterdam

Oh S.P., Nollett K.M., Madau P., et al. 2001, *ApJ*, 562, 10

Olive K. A., Skillman E., & Steigman G. 1997, *ApJ*, 483, 783

Panagia, N. 2002, in *Origins 2000: The heavy element trail from galaxies to habitable worlds*, ASP Conference Series, eds. Charles E. Woodward and Eric P. Smith, in press

Pauldrach A.W.A., Puls J., & Kudritzki R.P., 1986, *A&A* 164, 86

Pettini M. 2000, in *The First Stars, Proc. of the MPA/ESO Workshop held at Garching, 4-6 august 1999*, ESO Astrophysics Symposia, Springer, p. 303

Pettini M. 1999, in Chemical Evolution from Zero to High Redshift,
Proc. of the ESO workshop held in Garching, 14-16 October 1998,
eds. Walsh J.R., Rosa M.R., Springer, p. 223

Portinari L., Chiosi C., & Bressan A. 1998, A&A, 334, 505

Puls J., Springmann U., & Lennon M. 2000, A&AS, 141, 23

Salvaterra R., & Ferrara A. 2002, preprint

Scannapieco E., Ferrara A., & Madau P. 2002, ApJ, 574, 590

Schaerer D. 2002, A&A, 382, 28

Schwarzschild M., & Härm R. 1959, ApJ, 129, 637

Shi X. 1995, ApJ, 446, 637

Simon N.R., & Stothers R. 1970, A&A, 6, 183

Vink, J.S., de Koter, A., & Lamers, H.J.G.L.M., 2001, A&A, 369, 574

Weiss A., Abel T., & Hill V. (eds.), 2000, The First Stars, Proc. of
the MPA/ESO Workshop held at Garching, 4-6 august 1999, ESO
Astrophysics Symposia, Springer

Woosley S.E., & Weaver T.A. 1995, ApJS, 101, 181